

1 Original Research Article

2 4 **Development of Moisture Sorption Isotherm and** 5 **Mathematical Modeling of Finger Millet (*Eleusine coracana*)**

6 7 **Abstract**

In the literature, only a limited number of studies have explored the sorption characteristics of finger millet-based products. Moisture sorption isotherms provide information on the interaction between food and the storage environment. The sorption isotherms of finger millet based food product were studied with dynamic vapor sorption method, isopiestic Method and static gravimetric methods at different temperatures ranging from 25–70°C with humidity ranges from 5-100%. Additionally, no research has been conducted on whole grains concerning their storage for further processing. This study deals with the sorption properties of whole finger millet grains. Methodically, the equilibrium moisture content of whole finger millet grains was determined by the dynamic humidity chamber method. The Guggenheim–Andersen–de Boer (GAB), Brunauer–Emmett–Teller (BET), Henderson, and Halsey sorption models were applied to describe the relationship between detected water activity and equilibrium moisture content. The study was conducted at three different temperature levels of 25°C, 30°C, and 35°C. The relative humidity ranged from 10% to 90%, with an increment of 10%. The value of average R^2 for each model is 0.9103, 0.7226, 0.9123 and 0.8853, respectively. Furthermore, a new mathematical model incorporating exponential and power-law (nonlinear) relationships was developed, achieving an average R^2 value of 0.9720. Furthermore, this study validates the developed mathematical model for fitting sorption isotherms across different millet varieties and temperature levels. Experimental data from EX-BORNO millet were utilized for model validation. The results demonstrate high accuracy, with the coefficient of determination R^2 values for adsorption at 30°C, 40°C, 50°C, 60°C, and 70°C recorded as 0.976, 0.968, 0.963, 0.951, and 0.977, respectively. Similarly, the R^2 values for desorption at these temperatures were 0.978, 0.970, 0.963, 0.954, and 0.963. These findings confirm the robustness of the developed model in capturing moisture sorption behavior, providing a reliable tool for optimizing storage and processing conditions for millet. The developed mathematical model enhances the accuracy of moisture equilibrium predictions, facilitating the development of improved storage systems and drying strategies. These findings contribute to extending the shelf life and optimizing the processing efficiency of finger millet grains in the food industry. Additionally, this study offers a comprehensive analysis of the moisture sorption behavior of whole finger millet grains.

8
9 *Keywords: Adsorption, Desorption, Finger Millet, Moisture Content, Modeling [1mm]*

10 **1 Introduction**

11 Finger millet (*Eleusine coracana*), commonly known as raagi in India, is a highly nutritious cereal
12 crop predominantly cultivated in India and Africa. It serves as a rich source of dietary fiber, complex
13 carbohydrates, and essential amino acids such as methionine and tryptophan, contributing to its

14 significant role in food security and nutrition [Devi et al., 2014]. Moreover, finger millet is naturally
15 gluten-free, making it an ideal alternative for individuals with celiac disease or gluten sensitivity
16 [Shobana and Malleshi, 2007]. The grains of finger millet are typically ground into flour and utilized in
17 various culinary applications, including porridges, flatbreads, and baked goods.

18 Moisture content is a critical factor influencing the stability, quality, and shelf life of food materials.
19 It refers to the presence of water in a substance in different forms, including liquid, vapor, or absorbed
20 water. Controlling and measuring moisture levels are crucial in various industries such as food
21 production, pharmaceuticals and agriculture, as excessive or insufficient moisture can affect product
22 quality and microbial stability [Barbosa-Cánovas et al., 2020]. In food systems, moisture affects
23 textural properties, enzymatic reactions, and microbial growth, requiring precise moisture regulation to
24 prevent spoilage and ensure longevity. Sorption is a collective term encompassing both adsorption
25 and desorption processes. Adsorption refers to the adhesion of molecules onto the surface of a
26 material, whereas desorption describes the release of molecules from a material into the surrounding
27 environment [Iglesias and Chirife, 1976]. Understanding these processes is vital for assessing the
28 moisture interactions in food and biomaterials.

29 A sorption isotherm graphically represents the equilibrium moisture content of a material as a
30 function of water activity at a constant temperature [Labuza, 1984]. Moisture sorption isotherms are
31 widely used to determine the optimal storage conditions for food products, preventing spoilage, mold
32 growth, and other deterioration factors [Van den Berg and Bruin, 1978]. This knowledge enables
33 the development of effective packaging strategies to maintain product quality and extend shelf life.
34 Water activity, an essential indicator of food stability, helps assess microbial growth potential, oxidative
35 rancidity, and nonenzymatic reactions, ultimately determining the shelf stability of food products [Chirife
36 and Iglesias, 1978].

37 Sorption isotherm modeling has also been widely utilized to predict moisture behavior in food
38 systems. Traditional models such as BET and GAB have been applied to various grains, including rice
39 [Toğrul and Arslan, 2006] and pearl millet [Goneli et al., 2010], where equilibrium moisture content
40 decreased with increasing temperature. Advanced computational techniques, such as artificial neural
41 networks (ANNs), have been employed to predict moisture sorption behavior in cereals and legumes,
42 offering a robust alternative to complex iterative solutions [Al-Mahasneh et al., 2014]. Additionally,
43 moisture sorption characteristics have been linked to storage stability and product quality in extruded
44 food products, where the isotherms exhibited Type-II behavior at varying temperatures [Sahu and Patel,
45 2020]. The findings from above studies contribute significantly to optimizing food storage conditions,
46 enhancing product stability, and developing improved food packaging materials.

47 Hysteresis, a common phenomenon observed in sorption isotherms, occurs when the adsorption
48 and desorption curves do not coincide, resulting in a loop in the graphical representation. This behavior
49 is particularly evident in porous materials due to the complex interactions between adsorbate molecules
50 and the adsorbent surface [Lowell et al., 2012]. The International Union of Pure and Applied Chemistry
51 (IUPAC) classifies hysteresis into four types:

- 52 **a** H1 Type Hysteresis: Characterized by a closed loop with a sharp transition between adsorption and
53 desorption.
- 54 **b** H2 Type Hysteresis: Features a gradual desorption branch that does not entirely retrace the
55 adsorption path.
- 56 **c** H3 Type Hysteresis: Exhibits a wide loop with a desorption branch at higher relative pressures.
- 57 **d** H4 Type Hysteresis: Presents a narrow loop where the desorption branch partially follows the
58 adsorption path [Sing, 1985].

59 . Hysteresis occurs due to differences in the energy required for adsorption (moisture uptake) and
60 desorption (moisture release), often influenced by material structure, pore size, and interactions
61 between water molecules and the material [Van der Sman, 2023, Caurie, 2007, YORK, 1981, Yang
62 et al., 1997].

63 H1 hysteresis is characterized by a narrow, steep loop in the moisture sorption isotherm. This type
64 of hysteresis is typically observed in materials with uniform, cylindrical pores, such as well-ordered
65 mesoporous materials like Spray-dried dairy powders. The adsorption and desorption branches of
66 the loop are nearly parallel, indicating minimal pore network effects [Cychosz and Thommes, 2018].
67 This suggests that the material has a relatively simple and consistent pore structure, allowing for a
68 more predictable and reversible moisture sorption process.

69 H2 hysteresis exhibits a broader loop with a steep desorption branch. It is commonly found in
70 materials with complex pore networks viz. Starch-based foods . In these materials, desorption is
71 delayed due to pore blocking, which leads to a sharp drop in moisture content at a specific relative
72 humidity (RH). This behavior is a result of the intricate pore structure, where narrower pore openings
73 can trap moisture, causing a lag in desorption compared to adsorption [Shimizu and Matubayasi,
74 2024].

75 H3 hysteresis features a gradual, sloping loop without a clear plateau. This type of hysteresis
76 is often observed in materials with non-rigid aggregates or slit-shaped pores, such as dehydrated
77 fruits/vegetables or layered structures [Schiller et al., 2018]. The absence of a distinct plateau and the
78 sloping nature of the loop reflect weaker interactions between water and the material. This indicates
79 that the material's structure does not facilitate strong or uniform moisture retention, leading to a more
80 gradual change in moisture content with varying RH [Hong et al., 2018].

81 H4 hysteresis is exemplified by protein-rich foods such as casein or soy protein isolates. These
82 materials typically possess a combination of microporous and mesoporous structures. At low RH ,
83 moisture primarily fills the micropores, resulting in a narrow hysteresis loop. As the RH increases,
84 capillary condensation occurs in the larger mesopores, leading to a broader loop. This dual behavior,
85 characterized by a narrow loop at low RH and a broader loop at higher RH, is a hallmark of H4
86 hysteresis [Toncón-Leal et al., 2021].

87 Finger millet grains are susceptible to moisture, which can lead to spoilage, mold growth, and
88 nutrient loss [Nickhil et al., 2024]. Sorption isotherm studies aid in determining the appropriate storage
89 conditions (humidity levels, temperature, and packaging) to maintain the quality and prevent spoilage
90 during storage [Gichau et al., 2020]. Different foods have specific moisture content ranges where they
91 are more stable and less prone to spoilage or deterioration. For Finger millets, knowing the range of
92 moisture content at different humidity levels can help in preserving its nutritional value, taste, texture,
93 and overall quality during storage and processing [Balasubramanian and Viswanathan, 2010].

94 Studies on various finger millet-based foods as well other millets, including extruded products and
95 probiotic milk powder, have shown Type II or Type III isotherms [Yadav and Mishra, 2023]. The GAB
96 and BET models have been found to best fit the sorption data [Timmermann, 2003]. The sorption
97 isotherms of millet grains exhibit a sigmoidal shape (type II) and are influenced by temperature and
98 relative humidity [Alamri et al., 2018]. Various mathematical models, including GAB, BET, and modified
99 Henderson, have been used to describe the sorption behavior of millet grains and flours [Sharma et al.,
100 2018, Corrêa et al., 2006, Acurio et al., 2024].

101 Understanding sorption isotherms and hysteresis behavior in finger millet is crucial for optimizing
102 storage conditions, improving food processing techniques, and ensuring product stability. This study
103 aims to characterize the moisture sorption behavior of finger millet and evaluate the hysteresis effect
104 using a DTH-controlled chamber. In this study, a dynamic temperature-humidity (DTH) controlled
105 chamber was employed to measure the water sorption isotherm of finger millet. The temperature
106 and relative humidity within the DTH chamber were controlled within the range of 25°C to 35°C and
107 10% to 90%, respectively. This approach allows for precise measurement of water activity at various
108 conditions with high reproducibility. It also helps to design appropriate packaging materials and storage
109 conditions to prevent moisture uptake or loss during transportation and storage, ensuring the product

110 remains safe and maintains its quality.

111 2 Materials and Methods

112 Moisture sorption isotherms were determined using a controlled temperature-humidity chamber with
113 25°C, 30°C and 35°C of temperature levels and 10-90 % relative humidity levels. Samples were
114 equilibrated under different humidity conditions, and the equilibrium moisture content was measured.
115 The sorption data were analyzed using mathematical models to characterize the adsorption-desorption
116 behavior and hysteresis effects.

117 2.1 Material selection and Pre-processing

118 The GN8 variety of finger millet as shown in figure 1 was used in the experimental study. All foreign
119 materials, such as dust, stones, chaff, immature and broken seeds, as well as bad seeds, were
120 removed by winnowing and picking. Four replicates, each consisting of 5-gram samples, were
121 measured using an analytical weighing balance (Model No. MS-105, METLER TOLEDO, Readability-
122 0.01 mg; Repeatability-0.015 mg). A hot air oven (ModelNo. BTI 336, BIOTECHNOLOGIES INC.,
123 Temperature Sensitivity and accuracy- 0.5 °C) was used to measure the initial moisture content of the
finger millet grain.

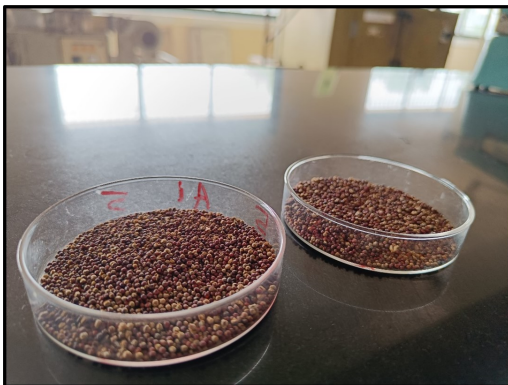


Figure 1: GN8 variety of Finger Millet



Figure 2: Dynamic temperature-humidity chamber

124 A humidity control chamber was used to create a controlled environment with temperatures of
125 25°C, 30°C, and 35°C, along with humidity levels of 10, 20, 30, 40, 50, 60, 70, 80, and 90% to study
126 the water sorption capacity of the samples. Desiccators were used to store samples during weighing.
127

128 A water activity meter was used to measure the water present in the samples when they attained
129 Equilibrium Moisture Content (EMC).

130 2.2 Moisture Content Determination

131 Initial moisture content of the sample was measured in quadruplicates by drying samples at 105°C for
132 24 h in a hot air oven. Three trials were conducted and statistical averaging taken to determine the
133 initial moisture content present in the sample. Moisture content was determined using equation 2.1.

$$Mc = (W_w - W_d) / W_d * 100 \quad (2.1)$$

134 where:

- 135 • Mc = moisture content (dry basis)
- 136 • W_w = weight of materials before oven drying
- 137 • W_d = weight of material after oven drying

138 2.3 Determination of Isotherms

139 In this developed method, a dynamic temperature-humidity (DTH) chamber (Model No. 106RP92C,
140 EIE INSTRUMENTS PVT. LTD.) as shown in figure 2 was used to measure the sorption isotherm.
141 DTH has preheating technology and a unique heating system that ensures homogeneous air and
142 temperature distribution inside a chamber. At the same time, this technology ensures fast recovery of
143 the humidity and temperature after opening and closing. In this technology, water spray in a premixing
144 chamber and mix with air (i.e., desired relative humidity) and then circulate to the humidity chamber at a
145 specified relative humidity. The air relative humidity and temperature are automatically controlled by
146 the system. The temperature and humidity of the chamber can be controlled in the range of 22°C to
147 70°C and 10 to 95 %, respectively. Finally, weight of the samples were recorded at time interval of 3
148 hours until equilibrium state achieved.

149 Initially, the DTH chamber was set to a temperature of 25°C with 10% relative humidity. The
150 samples, each weighing 5 grams, were placed inside the chamber only after it had stabilized at the
151 set conditions. The samples were uniformly distributed in four petri dishes. The weight of each
152 samples were recorded at 3 hours of intervals until equilibrium was reached. Subsequently, the relative
153 humidity of the chamber was increased to 20% while maintaining the temperature at 25°C, and the
154 weight of samples were recorded every 3 hours until equilibrium reached. This process was repeated
155 by incrementing the relative humidity by 10% steps up to 90% for the adsorption process. At each
156 equilibrium condition the water activity was measured.

157 Table 1 represents the adsorption isotherm data at different temperature levels 25°C, 30°C and
158 35°C with the corresponding EMC and water activity at various RH.

159 For isotherm measurements at different temperatures (30°C and 35°C), the same procedure
160 was followed. For the desorption process, the relative humidity of the chamber was reduced in
161 10% decrements from 90% to 10% at temperatures of 25°C, 30°C, and 35°C, following the same
162 methodology. Table 2 represents the desorption isotherm data at different temperature levels 25°C,
163 30°C and 35°C with the corresponding EMC and water activity at various RH.

164 2.4 Different Models of Sorption Isotherm

165 The collected isotherm data was analyzed and assessed using various well-established sorption
166 isotherm models that are commonly applied in moisture sorption studies. These models include the
167 GAB model, the Brunauer-Emmett-Teller (BET) model, the Henderson and the Halsey model. Each of

Table 1: Adsorption data at 25°C, 30°C and 35°C

RH (%)	25°C		30°C		35°C	
	EMC(%db)	Water Activity(a_w)	EMC(%db)	Water Activity(a_w)	EMC(%db)	Water Activity(a_w)
10	4.38	0.251	3.17	0.281	5.49	0.153
20	6.03	0.278	5.36	0.282	6.43	0.206
30	7.27	0.312	7.07	0.296	7.22	0.264
40	7.95	0.360	7.45	0.319	7.71	0.324
50	8.75	0.411	8.17	0.379	7.75	0.396
60	9.55	0.485	8.89	0.447	8.06	0.466
70	10.59	0.540	9.90	0.485	10.24	0.533
80	12.08	0.627	11.17	0.601	10.65	0.620
90	14.21	0.716	12.48	0.708	11.85	0.703

Table 2: Desorption data at 25°C, 30°C and 35°C

RH (%)	25°C		30°C		35°C	
	EMC(%db)	Water Activity(a_w)	EMC(%db)	Water Activity(a_w)	EMC(%db)	Water Activity(a_w)
10	2.08	0.239	2.33	0.282	5.86	0.084
20	4.19	0.272	4.44	0.284	6.39	0.162
30	6.33	0.313	6.35	0.301	7.02	0.240
40	7.95	0.360	7.50	0.321	7.70	0.319
50	9.85	0.423	7.97	0.389	7.73	0.392
60	11.45	0.475	8.93	0.459	8.05	0.472
70	12.33	0.554	10.0	0.500	8.97	0.554
80	12.96	0.628	11.79	0.606	10.41	0.621
90	14.19	0.715	12.48	0.789	11.81	0.703

168 these models was evaluated to determine its suitability in accurately describing the moisture sorption
 169 behavior of the finger millet.

170 2.4.1 GAB (Guggenheim-Anderson-de Boer) Model

171 The GAB model is best suited for food products, including grains and millets, as it accounts for
 172 monolayer moisture content, multilayer sorption, and sorption at higher water activities. It provides
 173 good accuracy over a wide range of water activity (0.10-0.90). GAB model can be express as below:

$$M = \frac{M_0 C K a_w}{(1 - K a_w)(1 - K a_w + C K a_w)} \quad (2.2)$$

174 where: - M = equilibrium moisture content (g water/g dry matter) - M_0 = monolayer moisture
 175 content - C = Guggenheim constant - K = factor correcting for multilayer adsorption - a_w = water
 176 activity

177 2.4.2 BET (Brunauer-Emmett-Teller) Model

178 The BET model is good for moisture sorption at low water activity (0.05-0.50) but underestimates
 179 sorption at higher RH. BET model is expressed mathematically as:

$$M = \frac{M_0 C a_w}{(1 - a_w)(1 + (C - 1)a_w)} \quad (2.3)$$

180 where: - M = equilibrium moisture content (g water/g dry matter) - M_0 = monolayer moisture
 181 content - C = BET constant

182 2.4.3 Henderson Model

183 The Henderson model is an empirical equation commonly used for grains and food products due to its
 184 simplicity in fitting experimental data. The Henderson model for moisture sorption isotherms is given
 185 by:

$$[-\ln(1 - a_w)]^n = kT^{-1}M \quad (2.4)$$

186 where: - a_w = water activity - M = equilibrium moisture content - T = temperature in Kelvin - k , n =
 187 model constants

188 2.4.4 Halsey Model

189 The Halsey model is suitable for high RH conditions and is frequently used in cereals and grains and
 190 millets.

$$M = A \left(\ln \frac{1}{a_w} \right)^B \quad (2.5)$$

191 where: a_w = water activity M = equilibrium moisture content A , B = model constants

192 To analyze the sorption behavior of finger millet, experimental data were fitted to various widely
 193 used adsorption isotherm models, including GAB, BET, Henderson, and Halsey. The adsorption
 194 parameters for each model were estimated at different temperatures ($25^\circ C$, $30^\circ C$, and $35^\circ C$). Table
 195 3 presents the computed model parameters, monolayer moisture content, and the corresponding
 196 goodness-of-fit measures, including the coefficient of determination (R^2), mean squared error (MSE),
 197 and mean absolute error (MAE). These parameters help in evaluating the accuracy and applicability of
 198 each model in predicting equilibrium moisture content under different temperature conditions.

Table 3: Adsorption Parameters for Different Models at Various Temperatures

Temperature ($^\circ C$)	Model	Monolayer Moisture	Constants	R^2	MSE	MAE
25	GAB	21.04	[21.04, 0.3171, 3.588]	0.97204	0.22922	0.39293
25	BET	4.4883	[4.488, 8.243e+05]	0.87423	1.03100	0.88004
25	Henderson	–	[12.38, 0.6292]	0.96565	0.28160	0.36283
25	Halsey	–	[7.516, 0.6141]	0.93328	0.54697	0.58871
30	GAB	135.61	[135.6, 0.1373, 0.9476]	0.79966	1.46270	1.05080
30	BET	4.2601	[4.26, 4.147e+05]	0.68270	2.31660	1.36310
30	Henderson	–	[11.62, 0.6025]	0.82256	1.29550	0.88858
30	Halsey	–	[7.2, 0.5831]	0.76857	1.68970	1.06870
35	GAB	6.4026	[6.403, 0.6807, 34.16]	0.95924	0.15896	0.31118
35	BET	4.2529	[4.253, 2.954e+06]	0.61109	1.51680	1.03910
35	Henderson	–	[10.77, 0.3789]	0.94886	0.19946	0.34426
35	Halsey	–	[7.76, 0.4235]	0.95431	0.17819	0.34823

199 Table 4 presents model parameters, monolayer moisture content, and goodness-of-fit measures
 200 (R^2 , MSE, MAE) to assess the accuracy of each model in predicting equilibrium moisture content at
 201 different temperatures for desorption behaviour.

202 All the selected sorption isotherm models were systematically evaluated, and their validation
 203 parameters were thoroughly analyzed in the Results and Discussion section. During the assessment,
 204 it was observed that there existed an opportunity to develop a more precise mathematical model

Table 4: Desorption Parameters for Different Models at Various Temperatures

Temperature (°C)	Model	Monolayer Moisture	Constants	R^2	MSE	MAE
25	GAB	327.93	[327.9, 0.2157, 0.2315]	0.87552	1.9318	1.2423
25	BET	5.008	[5.008, 11.42]	0.74284	3.9909	1.7204
25	Henderson	–	[13.23, 0.7531]	0.85591	2.2361	1.2372
25	Halsey	–	[7.334, 0.713]	0.77280	3.5259	1.5894
30	GAB	276.42	[276.4, 0.14, 0.4075]	0.74399	2.4773	1.4069
30	BET	3.5707	[3.571, 6.759e+05]	0.32087	6.5718	2.3508
30	Henderson	–	[10.8, 0.5714]	0.74997	2.4195	1.3240
30	Halsey	–	[6.946, 0.4833]	0.65199	3.3676	1.5319
35	GAB	5.5543	[5.554, 0.7402, 8.321e+04]	0.97327	0.086544	0.24708
35	BET	4.1491	[4.149, 1.313e+07]	0.49280	1.6425	1.1184
35	Henderson	–	[10.17, 0.2836]	0.88305	0.37871	0.5026
35	Halsey	–	[7.803, 0.3633]	0.96406	0.11637	0.30502

with an improved goodness-of-fit compared to the existing models. Consequently, a new exponential-power-based model was formulated specifically for finger millet to better describe its moisture sorption behavior. This newly developed model has the potential to be further validated and extended for application to other grains and millet varieties, ensuring broader applicability in food storage and processing studies.

3 Development of Mathematical Model

Mathematical modeling of moisture sorption isotherms is essential for understanding the equilibrium relationship between water activity and moisture content at different temperatures. Existing models such as GAB, BET, Halsey, and Henderson have been widely used; however, their accuracy varies depending on the material. To achieve a higher goodness-of-fit, a new exponential-power-based model was developed using MATLAB specifically for finger millet. This section presents the formulation of the developed model, its parameter estimation for selected temperature levels, and statistical validation to ensure its applicability in predicting sorption behavior.

The newly formulated mathematical model establishes a quantitative relationship between EMC and a_w across different temperatures. This model is designed to accurately describe the sorption behavior of the material and provide a reliable prediction of moisture equilibrium conditions under varying environmental conditions. The mathematical expression representing this relationship is given as follows:

$$M(T, a_w) = A(T) \cdot e^{B(T) \cdot a_w} + C(T) \cdot a_w^{D(T)} \quad (3.1)$$

where:

- $M(T, a_w)$ = Equilibrium Moisture Content (%db)
- T = Temperature (°C)
- a_w = Water Activity
- $A(T), B(T), C(T), D(T)$ are temperature-dependent coefficients.

3.1 Evaluation of Developed Model

The accuracy and reliability of the developed mathematical model were evaluated by comparing its predictions with experimentally obtained data at three different temperature levels. To assess the model's performance, the experimental moisture sorption data were fitted using the developed

232 model, and its effectiveness was quantified using statistical validation metrics such as the coefficient
233 of determination (R^2) and the root mean square error (RMSE). The following sections present the
234 fitted models along with their respective efficiency measures, demonstrating the model's suitability for
235 describing the equilibrium moisture content-water activity relationship.

236 The newly developed mathematical model describing the relationship between equilibrium moisture
237 content (M) and water activity (a_w) at different temperatures is presented as follows:

238 For a temperature of 25°C , the model is given by:

$$M(25^\circ\text{C}, a_w) = 4.512 \cdot e^{1.215 \cdot a_w} + 2.157 \cdot a_w^{0.895} \quad (3.2)$$

239 The accuracy of the model at 25°C was evaluated using statistical parameters. The coefficient
240 of determination (R^2) was found to be **0.9728**, indicating that 97.28% of the variation in equilibrium
241 moisture content is explained by the model. Additionally, the root mean square error (RMSE) was
242 **0.4722**, demonstrating a low prediction error and strong agreement between the experimental and
243 predicted values.

244 For a temperature of 30°C , the model takes the form:

$$M(30^\circ\text{C}, a_w) = 3.876 \cdot e^{1.101 \cdot a_w} + 1.995 \cdot a_w^{0.923} \quad (3.3)$$

245 At 30°C , the model exhibited an R^2 value of 0.9934, signifying an excellent fit with the experimental
246 data, while the RMSE was determined to be **0.2189**, further confirming the model's high predictive
247 capability and minimal deviation from observed values.

248 For a temperature of 35°C , the model is expressed as:

$$M(35^\circ\text{C}, a_w) = 5.225 \cdot e^{1.089 \cdot a_w} + 1.641 \cdot a_w^{0.812} \quad (3.4)$$

249 At 35°C , the model achieved an R^2 value of 0.9498, reflecting a strong correlation between
250 the predicted and experimental values. The RMSE for this temperature was **0.4427**, indicating an
251 acceptable level of accuracy in predicting equilibrium moisture content at this condition.

252 These results demonstrate the robustness of the developed model across different temperatures,
253 showing its potential applicability in predicting moisture sorption behavior with high precision.

254 3.2 Comparison of the Developed Model with Existing Moisture 255 Sorption Models

256 The developed mathematical model for EMC as a function of water activity (a_w) and temperature (T) is
257 not exactly the same as any standard available model such as BET, GAB, Henderson, Hasley, Peleg,
258 Chung-Pfost, or Oswin models.

259 The evaluation of the existing sorption isotherm models resulted in average coefficient of
260 determination (R^2) values of **0.9103**, **0.7226**, **0.9123**, and **0.8853**, respectively as indicated by table 3.
261 While these models provided reasonable fits to the experimental data, a newly developed mathematical
262 model exhibited superior performance, achieving an average R^2 value of **0.9720**. This indicates a
263 significant improvement in the predictive accuracy of the moisture sorption behavior, demonstrating
264 the effectiveness and reliability of the developed model for describing equilibrium moisture content at
265 different temperatures.

266 3.3 Validation of Model with different Dataset

267 For the validation of the developed mathematical model across different millet varieties and temperature
268 levels, data from Ex-Borno millet was utilized, as reported in the study by [Aviara et al., 2016] as shown
269 in table 5.

Table 5: Equilibrium Moisture Content (EMC) at Different Temperatures and Water Activities (a_w) of EX-BORNO Millet

Temperature	a_w	0.07	0.11	0.22	0.32	0.51	0.61	0.70	0.82	0.89	0.97
30°C	Ads EMC	14.4	17.1	22.0	23.3	23.8	24.0	25.7	27.0	31.6	35.3
	Des EMC	14.4	17.1	22.0	24.2	25.6	26.0	26.5	27.0	31.6	35.3
40°C	a_w	0.07	0.11	0.22	0.32	0.51	0.61	0.71	0.82	0.89	0.98
	Ads EMC	12.8	15.5	19.7	20.8	21.3	21.8	22.7	24.7	27.0	31.1
	Des EMC	12.8	15.5	19.7	22.1	22.9	23.3	23.9	24.7	27.4	31.1
50°C	a_w	0.07	0.11	0.21	0.31	0.50	0.60	0.70	0.81	0.89	0.96
	Ads EMC	10.0	13.4	17.2	17.8	18.2	19.0	19.7	21.5	24.5	27.3
	Des EMC	10.0	13.5	17.2	18.6	19.7	20.6	21.5	24.6	27.3	–
60°C	a_w	0.07	0.11	0.21	0.31	0.50	0.60	0.70	0.80	0.88	0.95
	Ads EMC	8.5	11.5	14.9	16.9	17.0	17.4	17.5	18.7	21.5	25.0
	Des EMC	8.5	11.5	15.9	16.9	17.1	17.5	17.8	18.7	21.5	25.0
70°C	a_w	0.07	0.11	0.20	0.30	0.50	0.60	0.70	0.80	0.88	0.94
	Ads EMC	7.0	10.0	11.5	11.9	12.3	12.7	13.9	16.1	19.2	22.3
	Des EMC	7.0	10.0	12.9	14.0	14.6	15.0	15.5	16.4	19.3	22.3

3.4 Characteristics of Developed Model

The developed mathematical model possesses distinct characteristics, which are discussed in detail below. These features differentiate it from existing models.

1. Combination of Exponential and Power Law Terms

- The model consists of both an **exponential** term ($A(T)e^{B(T)a_w}$) and a **power-law** term ($C(T)a_w^{D(T)}$).
- Most existing models, such as BET and GAB, rely on thermodynamic principles and do not follow this hybrid functional form.

2. Temperature-Dependent Parameters

- In classical models like the Henderson equation:

$$EMC = \left(-\frac{\ln(1 - a_w)}{K} \right)^{\frac{1}{N}}$$

the parameters K and N are constants for a given material.

- In the developed model, the parameters $A(T)$, $B(T)$, $C(T)$, and $D(T)$ explicitly depend on temperature, making it more flexible.

3. Hybrid Model Structure

- The first term, $A(T)e^{B(T)a_w}$, captures exponential moisture sorption behavior.
- The second term, $C(T)a_w^{D(T)}$, accounts for nonlinear water activity dependency, which is often missing in purely empirical models.

287

- This combination allows better flexibility in fitting experimental sorption data.

288

The developed model is a **new empirical equation** developed by directly fitting to experimental data at different temperatures. It is **not the same** as existing models but shares some general characteristics with traditional moisture sorption models in food engineering.

289

290

291 4 Results and Discussions

292

The adsorption isotherm at each temperature level is shown in figure 3 for 25°C, figure 4 for 30°C and figure 5 for 35°C. The data points (red circles) represent experimental measurements, while the different curves correspond to various sorption models: GAB, BET, Henderson, and Halsey.

293

294

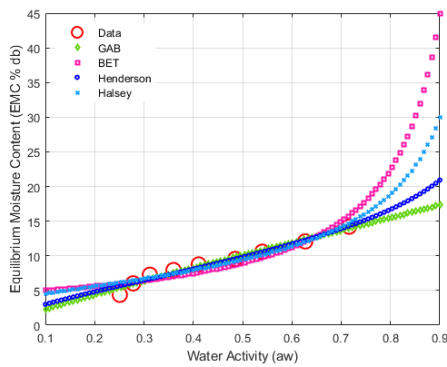


Figure 3: Moisture adsorption isotherm at 25°C

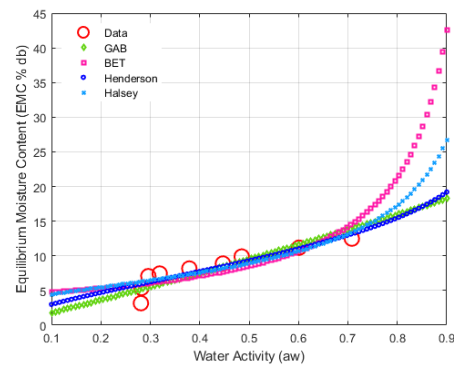


Figure 4: Moisture adsorption isotherm at 30°C

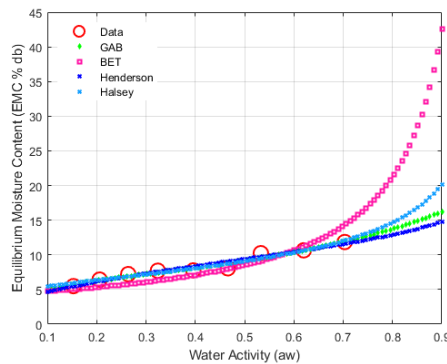


Figure 5: Moisture adsorption isotherm at 35°C

295

The GAB model (green diamonds) shows good agreement with experimental data across the entire range, while the BET model (pink squares) diverges significantly at higher water activity, overestimating

296

297 EMC. The Henderson and Halsey models (blue markers) follow the trend of the experimental data
298 more closely than BET but slightly deviate at higher a_w values.

299 From the figure 3 to figure 5, there is an improvement in the model fit, particularly for the GAB,
300 Henderson, and Halsey models. The GAB model remains the most accurate, aligning well with the
301 experimental data throughout. The BET model consistently exhibits an exponential rise in EMC at high
302 a_w values, suggesting its limitation for high water activity ranges. The Henderson and Halsey models
maintain a reasonable fit but still show some deviation from the data at high a_w .

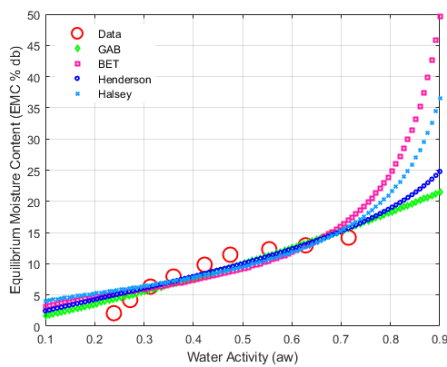


Figure 6: Moisture desorption isotherm at 25°C

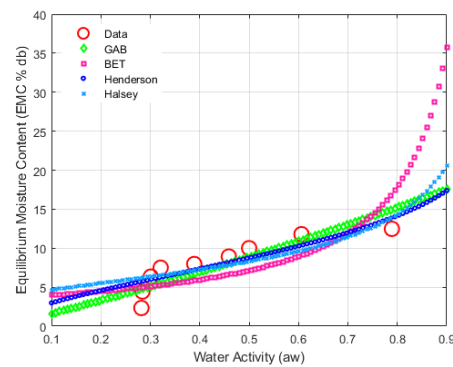


Figure 7: Moisture desorption isotherm at 30°C

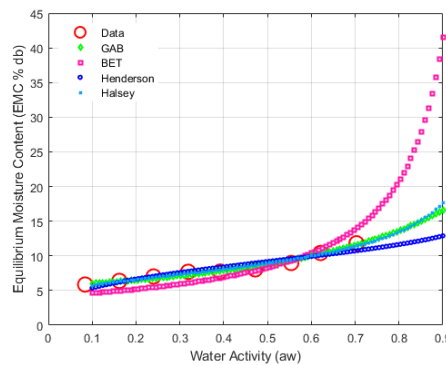


Figure 8: Moisture desorption isotherm at 35°C

303 The desorption isotherm at each temperature level is shown in figure 6 for 25°C, figure 7 for 30°C
304 and figure 8 for 35°C. The BET model (pink squares) shows a sharp increase at higher a_w , indicating
305 its limitation in accurately representing moisture content beyond monolayer adsorption.

306 The Henderson and Halsey models (blue markers) offer reasonable approximations but deviate
307 significantly at high a_w levels.

308 The results highlight the superiority of the GAB model for predicting moisture sorption behavior,
309 especially for food materials where water activity extends across a wide range. The BET model is only
310

311 suitable for lower a_w values, as it significantly overestimates EMC beyond 0.6 a_w . The Henderson and
312 Halsey models provide a moderate fit but are not as reliable as GAB.

313 The model's effectiveness has been evaluated with experimental data at three temperature levels
314 (25°C, 30°C, and 25°C), with corresponding equations explicitly stated. The statistical validation,
315 including R^2 and RMSE values, confirms the model's capability, with an average R^2 of 0.9720,
316 significantly outperforming existing models such as BET, GAB, and Henderson. The R^2 , demonstrated
317 through model evaluation across different temperatures, highlights its reliability in accurately describing
318 equilibrium moisture content.

319 To validate the developed mathematical model for various millet varieties and temperature levels,
320 the study utilized data from EX-BORNO millet, as reported by [Aviara et al., 2016]. The validation
321 results, as illustrated in figure 9, indicate that for different temperatures, namely 30°C, 40°C, 50°C,
322 60°C, and 70°C, the coefficient of determination (R^2) values for adsorption are 0.976, 0.968, 0.963,
323 0.951, and 0.977, respectively, while for desorption, the corresponding R^2 values are 0.978, 0.970,
324 0.963, 0.954, and 0.963 for EX-BORNO millet.

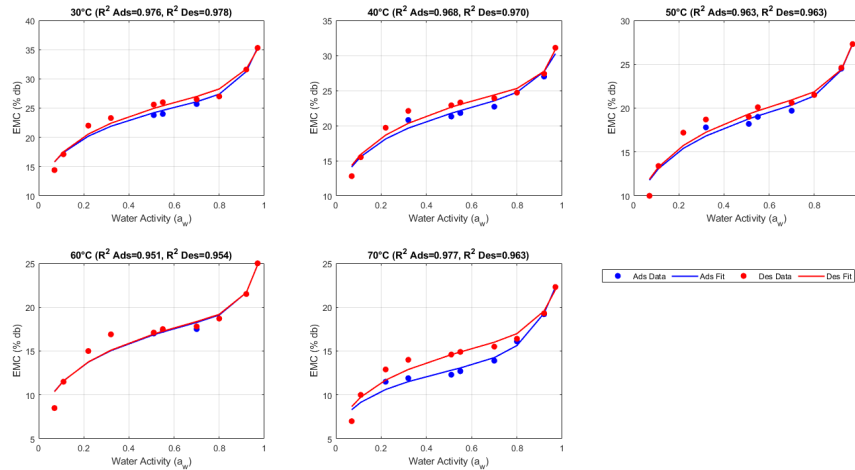


Figure 9: Validation of developed mathematical model with different temperature for EX-BORNO millet

325 Comparisons with traditional models reinforce the originality of this study, as the developed
326 model uniquely integrates exponential and power-law terms, making it distinct from standard moisture
327 sorption equations. These findings emphasize the importance of selecting the appropriate model when
328 analyzing sorption behavior in food products.

329 5 CONCLUSIONS

330 The study confirms the superiority of the GAB model in predicting moisture sorption behavior,
331 particularly for food materials with a wide range of water activity. While the BET model performs well
332 at lower a_w values, it significantly overestimates EMC beyond 0.6 a_w , limiting its applicability. The
333 Henderson and Halsey models offer a moderate fit but lack the reliability of the GAB model, making
334 them less suitable for accurate moisture sorption predictions.

335 The developed model introduces a hybrid approach to predict EMC by combining exponential
336 and power-law terms. Unlike conventional models such as BET and GAB, which are based on
337 thermodynamic principles, this model incorporates temperature-dependent parameters for improved
338 flexibility. The exponential term accounts for moisture sorption behavior, while the power-law term
339 captures nonlinear water activity effects. This structure enables better adaptability to experimental
340 data, making the model more versatile in describing moisture sorption characteristics across different
341 temperature conditions.

342 The evaluation of existing sorption isotherm models yielded average R^2 values of 0.9103, 0.7226,
343 0.9123, and 0.8853 for GAB, BET, Henderson and Halsey models, respectively. While these models
344 provided reasonable fits, the developed model outperformed them with an average R^2 of 0.9720,
345 demonstrating superior accuracy and reliability in describing moisture sorption behavior across
346 temperatures.

347 The validation results, based on an external dataset, demonstrate a strong correlation between
348 predicted using developed model and experimental values considered for EX-BORNO millet. The
349 coefficient of determination R^2 for adsorption at different temperatures (30°C , 40°C , 50°C , 60°C ,
350 and 70°C) are 0.976, 0.968, 0.963, 0.951, and 0.977, respectively. Similarly, for desorption, the
351 corresponding R^2 values are 0.978, 0.970, 0.963, 0.954, and 0.963. These results confirm the
352 accuracy and reliability of the proposed mathematical model across varying temperature conditions
353 and for different millets.

354 Acknowledgment

355 The authors are grateful to Anand Agricultural University for providing facilities to conduct the
356 experiment. The authors would like to thank the editor and anonymous reviewers for their comments
357 that help improve the quality of this work.

358

359 References

- 360 Liliana Acurio, Diego Salazar, María Eugenia García, Purificación García-Segovia, Javier Martínez-
361 Monzó, and Marta Igual. Characterization, mathematical modeling of moisture sorption isotherms
362 and bioactive compounds of andean root flours. *Current Research in Food Science*, 8:100752,
363 2024.
- 364 Majdi Al-Mahasneh, Fahad Alkoaik, Ahmed Khalil, Ahmad Al-Mahasneh, Ahmed El-Waziry, Ronnel
365 Fulleros, and Taha Rababah. A generic method for determining moisture sorption isotherms of
366 cereal grains and legumes using artificial neural networks. *Journal of Food Process Engineering*,
367 37(3):308–316, 2014.
- 368 MS Alamri, AA Mohamed, S Hussain, MA Ibraheem, and Akram A Abdo Qasem. Determination of
369 moisture sorption isotherm of crosslinked millet flour and oxirane using gab and bet. *Journal of*
370 *Chemistry*, 2018(1):2369762, 2018.
- 371 Ndubisi A Aviara, John O Ojediran, U Marwan Sa'id, and Abdulganiy O Raji. Effect of moisture
372 sorption hysteresis on thermodynamic properties of two millet varieties. *Agricultural Engineering*
373 *International: CIGR Journal*, 18(1):363–383, 2016.
- 374 S Balasubramanian and R Viswanathan. Influence of moisture content on physical properties of minor
375 millets. *Journal of food science and technology*, 47:279–284, 2010.
- 376 Gustavo V Barbosa-Cánovas, Anthony J Fontana Jr, Shelly J Schmidt, and Theodore P Labuza. *Water*
377 *activity in foods: fundamentals and applications*. John Wiley & Sons, 2020.

-
- 378 Matthew Caurie. Hysteresis phenomenon in foods. *International Journal of Food Science and*
379 *Technology*, 42(1):45–49, 2007.
- 380 Jorge Chirife and Hector A Iglesias. Equations for fitting water sorption isotherms of foods: Part 1—a
381 review. *International Journal of Food Science & Technology*, 13(3):159–174, 1978.
- 382 Paulo C Corrêa, Paulo C A Júnior, Deise M Ribeiro, and Fabrício S da Silva. Equilíbrio higroscópico
383 de milho, alpiste e painço: obtenção e modelagem. *Revista Brasileira de Engenharia Agrícola e*
384 *Ambiental*, 10:162–167, 2006.
- 385 Katie A Cychosz and Matthias Thommes. Progress in the physisorption characterization of nanoporous
386 gas storage materials. *Engineering*, 4(4):559–566, 2018.
- 387 Palanisamy Bruntha Devi, Rajendran Vijayabharathi, Sathyaseelan Sathyabama,
388 Nagappa Gurusiddappa Malleshi, and Venkatesan Brindha Priyadarisini. Health benefits
389 of finger millet (*eleusine coracana* L.) polyphenols and dietary fiber: a review. *Journal of food*
390 *science and technology*, 51:1021–1040, 2014.
- 391 Anne Wanjiru Gichau, Judith Kanensi Okoth, and Anselimo Makokha. Moisture sorption isotherm and
392 shelf life prediction of complementary food based on amaranth–sorghum grains. *Journal of food*
393 *science and technology*, 57:962–970, 2020.
- 394 André Luis Duarte Goneli, Paulo Cesar Corrêa, Gabriel Henrique Horta De Oliveira, Cassandra Ferreira
395 Gomes, and Fernando Mendes Botelho. Water sorption isotherms and thermodynamic properties
396 of pearl millet grain. *International journal of food science & technology*, 45(4):828–838, 2010.
- 397 Seongwon Hong, Kyle De Bruyn, Eric Bescher, Chris Ramseyer, and Thomas H-K Kang. Porosimetric
398 features of calcium sulfoaluminate and portland cement pastes: testing protocols and data analysis.
399 *Journal of Structural Integrity and Maintenance*, 3(1):52–66, 2018.
- 400 HA Iglesias and J Chirife. Prediction of the effect of temperature on water sorption isotherms of food
401 material. *International journal of food science & technology*, 11(2):109–116, 1976.
- 402 Theodore Peter Labuza. Moisture sorption: practical aspects of isotherm measurement and use. (*No*
403 *Title*), 1984.
- 404 Seymour Lowell, Joan E Shields, Martin A Thomas, and Matthias Thommes. *Characterization of*
405 *porous solids and powders: surface area, pore size and density*, volume 16. Springer Science &
406 Business Media, 2012.
- 407 C Nickhil, Raj Singh, Sankar Chandra Deka, and R Nisha. Exploring finger millet storage: an in-depth
408 review of challenges, innovations, and sustainable practices. *Cereal Research Communications*,
409 pages 1–23, 2024.
- 410 Chandrasah Sahu and Shadanan Patel. Moisture sorption characteristics and quality changes during
411 storage in defatted soy incorporated maize-millet based extruded product. *Lwt*, 133:110153, 2020.
- 412 Peter Schiller, Mirco Wahab, Thomas A Bier, and Hans-Jörg Mögel. Low pressure hysteresis in
413 materials with narrow slit pores. *Colloids and Interfaces*, 2(4):62, 2018.
- 414 Nitya Sharma, SK Goyal, Tanweer Alam, Sana Fatma, and Keshavan Niranjan. Effect of germination
415 on the functional and moisture sorption properties of high-pressure-processed foxtail millet grain
416 flour. *Food and bioprocess technology*, 11:209–222, 2018.

-
- 417 Seishi Shimizu and Nobuyuki Matubayasi. Sorption hysteresis: A statistical thermodynamic fluctuation
418 theory. *Langmuir*, 40(22):11504–11515, 2024.
- 419 S Shobana and NG Malleshi. Preparation and functional properties of decorticated finger millet
420 (eleusine coracana). *Journal of Food Engineering*, 79(2):529–538, 2007.
- 421 Kenneth SW Sing. Reporting physisorption data for gas/solid systems with special reference to the
422 determination of surface area and porosity (recommendations 1984). *Pure and applied chemistry*,
423 57(4):603–619, 1985.
- 424 Ernesto O Timmermann. Multilayer sorption parameters: Bet or gab values? *Colloids and Surfaces A:
425 Physicochemical and Engineering Aspects*, 220(1-3):235–260, 2003.
- 426 H Toğrul and N Arslan. Moisture sorption behaviour and thermodynamic characteristics of rice stored
427 in a chamber under controlled humidity. *Biosystems Engineering*, 95(2):181–195, 2006.
- 428 Cristian Fabian Toncón-Leal, Jhonny Villarroel-Rocha, MTPda Silva, Tiago Pinheiro Braga, and
429 K Sapag. Characterization of mesoporous region by the scanning of the hysteresis loop in
430 adsorption–desorption isotherms. *Adsorption*, 27(7):1109–1122, 2021.
- 431 C Van den Berg and S Bruin. Water activity and its estimation in food systems. In *Proceedings Int.
432 Symp. Properties of Water in Relation to Food Quality and Stability, Osaka, 1978*, 1978.
- 433 RGM Van der Sman. Effects of viscoelasticity on moisture sorption of maltodextrins. *Food
434 Hydrocolloids*, 139:108481, 2023.
- 435 Shweta Yadav and Sabyasachi Mishra. Moisture sorption isotherms and storage study of spray-dried
436 probiotic finger millet milk powder. *Journal of Stored Products Research*, 102:102128, 2023.
- 437 W Yang, S Sokhansanj, S Cenkowski, J Tang, and Y Wu. A general model for sorption hysteresis in
438 food materials. *Journal of food engineering*, 33(3-4):421–444, 1997.
- 439 PETER YORK. Analysis of moisture sorption hysteresis in hard gelatin capsules, maize starch, and
440 maize starch: drug powder mixtures. *Journal of Pharmacy and Pharmacology*, 33(1):269–273,
441 1981.